第31卷第5期
2012年10月

红外与毫米波学报
J. Infrared Millim. Waves

Vol. 31, No. 5
October, 2012

文章编号:1001-9014(2012)05-0389-05

DOI:10.3724/SP.J.1010.2012.00389

Passively Cr^{4+}:YAG Q-switched single-longitudinal-mode Nd:YAG laser with volume Bragg grating output mirror

REN De-Ming, QIAN Li-Ming, ZHAO Wei-Jiang, QU Yan-Chen, LIU Yuan-Ye, BAI Yan, CHEN Zhen-Lei

(National key Laboratory of Tunable Laser Technology, Harbin Institute of Technology, Harbin 150001, China)

Abstract: Taking Cr^{4+}:YAGs as saturable absorbers and reflective volume Bragg gratings (RVBG) as output mirror, passively Q-switched operation of flash-lamp pumped Nd:YAG single-longitudinal-mode (SLM) laser was demonstrated. Single-frequency operation is accomplished for all output powers by twisted mode cavity and RVBG. This method can bring higher energy and stability. The maximum linewidth of SLM laser is about 78 MHz. The curve of energy and pulse width have been obtained under conditions of several Cr^{4+}:YAGs with different initial transmissivity. The maximum SLM laser output energy is 20.8 mJ, minimum pulse duration is 13.2 ns and peak power is 1.18 MW.

Key words: single-longitudinal-mode; passively-Q, Cr^{4+}:YAG; Nd:YAG; reflective volume Bragg grating

PACS: 42.55.Rz

体光栅输出被动 Cr^{4+}:YAG 调 Q 单纵模 Nd:YAG 激光器研究

任德明, 钱黎明, 赵卫疆, 曲彦臣, 刘原野, 白 岩, 陈振雷

(哈尔滨工业大学 可调谐(气体)激光国防科技重点实验室,黑龙江 哈尔滨 150001)

摘要: 以 Cr^{4+}:YAG 为饱和吸收体,体布拉格光栅为耦合输出窗,研究了被动调 Q 闪光灯泵浦 Nd:YAG 单纵模激光器. 通过扭转模腔和体布拉格光栅相结合的方式获得单纵模输出,提高了单纵模输出能量及稳定性. 对于不同初始透过率的 Cr^{4+}:YAG 晶体,得到了单纵模输出能量和脉宽的曲线. 单纵模激光最大线宽约为 78 MHz. 最大单纵模单脉冲输出能量为 20.8 mJ,最小的脉宽为 13.2 ns,最大峰值功率为 1.18 MW.

关 键 词: 单纵模;被动调 Q;Cr^{4+}:YAG;Nd:YAG;反射式体布拉格光栅

中图分类号: O432.1 **文献标识码**: A

Introduction

Q-switched SLM lasers in a nanosecond regime with a stable repetition rate are widely used in applications such as laser remote sensing, laser satellite networking, laser communication, and many nonlinear optical experiments[1]. Laser diode (LD) pumped passively Q-switched (PQ) laser has been studied generally because of its high efficiency. However it is limited in some field because of its low peak power of laser pulse[2]. Most of applications require additional properties of the Q-switched lasers, such as SLM, single transverse mode (STM), stable pulse shape and pulse width, or ultra-compact and rugged oscillators with some, or all, of the above properties[3].

Longitudinal mode selection, which requires both narrow line width and easy to achieve, is of significance in the SLM system. The wavelength selectivity system can be described as spectral selector. Laser cavity designed for a SLM is usually based on spectral selectors which contain multiple dispersive elements [4]. The SLM laser only operates about threshold of laser with common methods because of mode competition, namely the output energy is low. The higher SLM energy and stability is the goal of researchers. A new type of longitudinal mode selector for solid state lasers has been proposed. This approach is based on intra-cavity mode selection by using volume Bragg grating (VBG) recorded on photo-thermo-refractive (PTR) glass [5-6]. The RVBG

Received date: 2011-05-23, **revised date**: 2012-07-13 **收稿日期**:2011-05-23, **修回日期**:2012-07-13

Foundation items: Supported by "the Fundamental Research Funds for the Central Universities" (Grant No. HIT.KOLF.2010036).

Biography: REN De-ming (1968-), male, Hebei, Professor, research field is solid state laser. E-mail: co2@hit.edu.cn.

works as output coupler in CW, pulsed solid state and semiconductor lasers. It can bring very excellent performance in SLM laser system.

1 Experimental setup

In the experiment, a RVBG is added into the twisted mode cavity for both mode selection and stabilization of SLM The typical twisted mode cavity core is composed of two quarter wave plates and a polarizer[7]. Based on Kogelnik's theory [8], Ciapurin derived the relationship between diffraction efficiency of RVBG and the detuning from center wavelength [9].

$$\eta = \left[1 + \frac{1 - \left(\frac{\lambda f^2 \Delta\lambda}{2 n_{av} \delta_n}\right)^2}{\sinh^2 \sqrt{\left(\frac{2\pi n_{av} d \delta_n}{\lambda^2 f}\right)^2 - \left(\frac{\pi f d \Delta\lambda}{\lambda}\right)^2}} \right]^{-1}, \quad (1)$$

where n_{av} denotes the average refractive index of the grating, δ_n represents the index modulation, d is the thickness of grating, f is the spatial frequency of grating modulation, λ is the wavelength of laser, $\Delta\lambda$ represents the detuning from center wavelength.

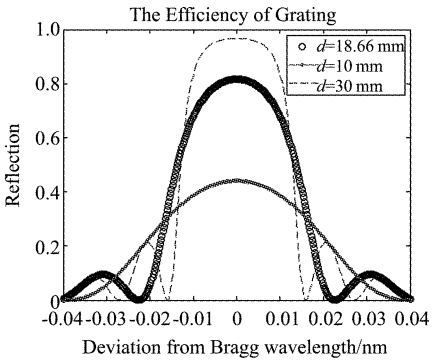

Fig. 1 The relation between diffraction efficiency and the error of central wavelength
图1 衍射效率和入射激光波长的关系

The diffraction efficiency of RVBG is shown in Fig. 1, where central wavelength is at 1 064.4 nm. The spatial frequency of the grating is 2 793 mm^{-1}, the average refractive index is 1.49 with a modulation of 2.7×10^{-5}. The thickness of RVBG, which plays an important role in high reflectivity and narrow bandwidth, is the only variable in our mathematical model.

In order to achieve a stable SLM laser, twisted mode cavity and RVBG are employed in oscillator, as shown in Fig. 2. The RVBG used in this experiment with narrow spectral selectivity was designed mainly for longitudinal mode selection. The spectral profile of the diffraction efficiency of RVBG centered at ~ 1064.4 nm is shown in Fig. 3. The RVBG has bandwidth (FWHM) of about 0.05 nm along with the maximum diffraction efficiency of 90.6% as shown in Fig. 3. The physical dimension of RVBG is 8.0 mm x 6.2 mm x 18.66 mm. The important feature of RVBG is that diffraction efficiency strongly depends on incident wavelength. Other wavelengths have big losses except the center wavelength. So it is easy to get the higher diffraction efficiency around the centre wavelength. Therefore, a SLM laser can be achieved. The schematic diagram of the PQ Nd:YAG SLM laser is shown in Fig. 2. The Nd:YAG laser cavity mainly consists of five parts: a total reflection mirror (TRM), a twisted mode selector, passively Q-switched crystal, an adjustable aperture for transverse mode selection and a RVBG as an output coupler. The total reflectivity of the flat end mirror is greater than 99%. The Nd:YAG crystal, the dimension of which is 5-mm in diameter and 80 mm in length, pumped by a single flash-lamp. And the doped concentration is 1%. The Nd:YAG is cooled by water about 20 ℃. The twisted mode include two 1/4 wave-plates at 1 064 nm and a polarizing disc which is laid by Brewster angle. Total optical length of laser was about 22.5 cm. The Cr^{4+}:YAG saturable absorber was laid near the total reflection mirror. Q-switched pulses were readily observed with an energy detector, PIN photodiode and digital oscilloscope.

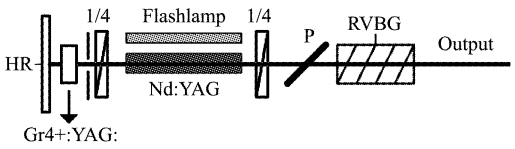

Fig. 2 Schematic of passively Cr^{4+}:YAG Q-switched Nd:YAG SLM laser pumped by flash lamp
图2 闪光灯泵浦 Cr4 + YAG 被动调 Q 单纵模 Nd:YAG 激光器结构图

2 Data analyzation

Nine different Cr^{4+}:YAG absorbers with nine different initial transmissivity are shown in Table. 1. The tenth parameter with initial transmissivity 100%

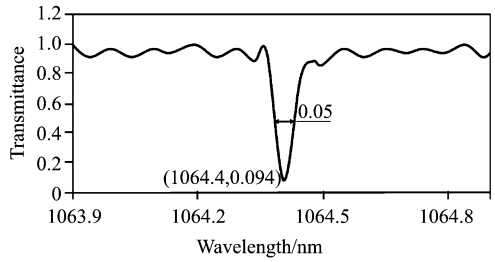

Fig. 3　The transmissivity of the RVBG depends on wavelength
图 3　体布拉格光栅透过率和波长关系

means that there is no Q-crystal in the cavity. The energy, pulse width and peak power results under different conditions were studied. The highest SLM energy 20.8 mJ was obtained with the absorber having 79.5% initial transmissivity and narrowest SLM pulse- width 13.2 ns was obtained with the absorber having 21.7% initial transmissivity. The maximum peak power is about 1.18 MW.

Table 1　The serial numbers of different initial transmissivity of Cr^{4+}:YAG
表 1　不同的 Cr^{4+}:YAG 初始透过率值

Number	1	2	3	4	5	6	7	8	9	10
Transmissivity(%)	21.7	30.4	35.2	46.7	50.4	56	64.8	72.7	79.5	100

The energy of laser as shown in Fig. 4 was detected by detector (Newport 818E). The switched pulse energy changes obviously under the conditions of different Cr^{4+}:YAG with different initial transmissivity. The prime reason is that threshold of laser cavity has been changed for different Cr^{4+}:YAG. Other reasons may be the unstability of laser cavity, cooling water and flash lamp as shown in Fig. 2. the laser output can no longer stabilize the central lasing mode at higher pump energy. In the experiment, the multimode emission occurs when the pump power exceeds 115% of the threshold. The fifth Cr^{4+}:YAG is unusual because of its low energy output. Some exiguous cracks was found in this piece of Cr^{4+}:YAG after very careful examination. The crack is too tiny to show them in pictures. At each measurement, we record twenty energy data were recorded in sequence and the standard error is analyzed with Origin 8.5.

The spectrum of laser wasmeasured by the method of F-P photographic process using two lenses, an F-P

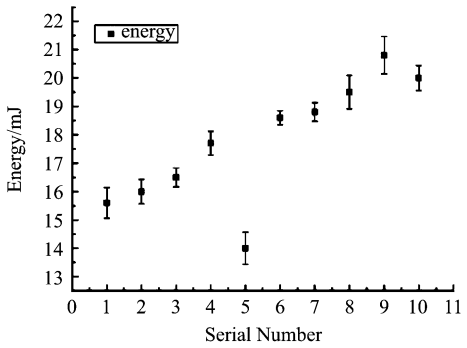

Fig. 4　The energy of SLM laser output with different Cr^{4+}:YAG
图 4　不同 Cr^{4+}:YAG 的单纵模激光输出能量

etalon and a CCD as shown in Fig. 5. In experiment, the F-P has 18.7 pm free spectral range at $\lambda = 1\ 064$ nm. The physical dimension of F-P is 2 cm at length and 2.5 cm in diameter. In experiment the material of etalon is BK7 glass with refractive index 1.506 1 at the wavelength 1 064 nm. The free-spectral range of the etalon is 4.98 GHz corresponds to 18.7 pm in wavelength. The two lenses were used to produce interference fringes on the surface of CCD camera. The focus of lens 1 is 30 mm and the lens 2 is 100 mm. The sensitive dimension of CCD is 7.6 mm × 6.2 mm. And the line width of laser can also be measured by the CCD system [10]. The interference fringes shown in Fig. 6 indicate that the laser operates at SLM. The maximum linewidth of SLM laser is about 78 MHz based on the method in Ref. 10.

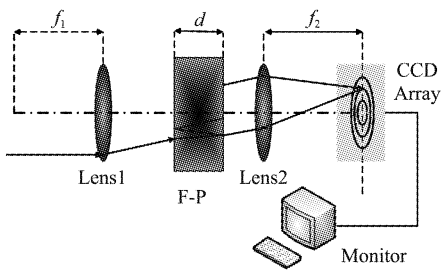

Fig. 5　The structure scheme of displaying SLM and linewidth of laser
图 5　单纵模和线宽测量装置结构图

The typical normalized waveform of laser pulse with the first Cr^{4+}:YAG and the pulse width is 13.2 ns was shown in Fig. 7. The waveforms of pulse under other Cr^{4+}:YAG are similar. The pulse width decrease

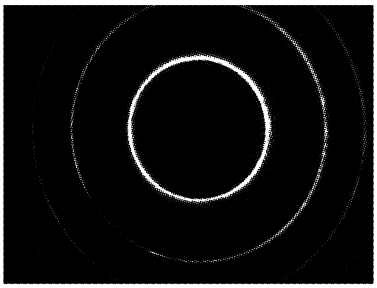

Fig. 6 Interference ring of SLM
图6 单纵模干涉环

when the initial transmissivity of Cr^{4+}:YAG increase as shown in Fig. 8. The narrowest pulse duration is 13.2 ns. At each measurement, ten energy data were recorded in sequence and the standard error is analyzed with Origin 8.5 too.

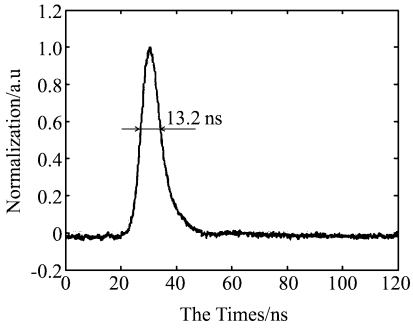

Fig. 7 The normalized waveform of laser pulse
图7 激光输出脉冲波形

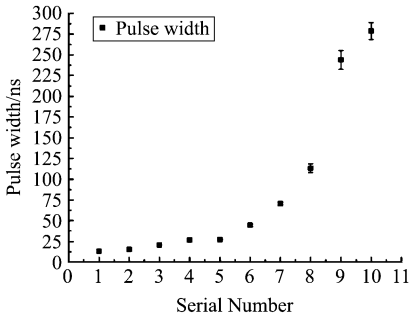

Fig. 8 Pulse duration of SLM laser output with different Cr^{4+}:YAG
图8 不同 Cr^{4+}:YAG 的单纵模激光脉宽

The peak power shown in Fig. 9 is calculated from the energy and pulse width. The peak power decreases following the decrease of the initial transmissivity of Cr^{4+}:YAG. The fifth is unusual too.

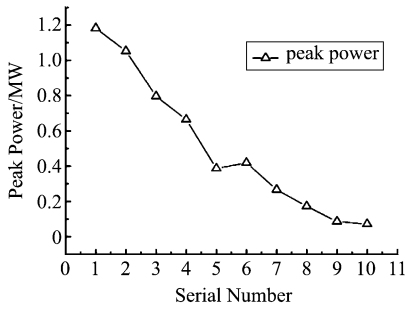

Fig. 9 Peak power of SLM laser output with different Cr^{4+}:YAG
图9 不同 Cr^{4+}:YAG 的单纵模激光峰值功率

3 Conclusions

In conclusion, the operation of a flash lamp pumped Nd:YAG SLM laser passively Q-switched by Cr^{4+}:YAGs saturable absorber was described. Along with the common structure-twisted mode cavity, the high-precision spectral selective character of RVBG can bring high energy and stability of SLM laser output. The maximum linewidth of SLM laser is about 78 MHz. This maximum energy of laser is 20.8 mJ, minimum pulse width 13.2 ns and maximum peak power 1.18 MW at 1 Hz repetition rates.

With good stability in terms of energy and frequency fluctuations, the extremely narrow lasing line width will be achieved on condition that the compact and robust design is finished. Then it is an interesting device for applications such as Lidar systems and nonlinear optics.

REFERENCES

[1] Giovanni Martucci, Renaud Matthey, Valentin Mitev, *et al*. Frequency of Boundary-Layer-Top Fluctuations in Convective and Stable Conditions using Laser Remote Sensing[J]. *Boundary-LayerMeteorol*. 2010,**135**(2): 313-331.

[2] YanFeng, JianrenLu, KazunoriTakaichi, *et al*. Passively Q-switched ceramic Nd^{3+}:YAG Cr^{4+}:YAG lasers[J]. *APPLIED OPTICS*. 2004, **43**(14): 2944-2947.

[3] KristoferY Shrestha, K. Clint Slatton, WilliamE. Carter, *et al*. Performance Metrics for Single-Photon Laser Ranging [C]. IEEE GEOSCIENCE AND REMOTE SENSING LETTERS, 2010, **7**(2):338-342.

[4] Bjorn Jacobsson, Valdas Pasiskevicius, Fredrik Laurell. Single- longitudinal- mode Nd-laser with a Bragg-grating Fabry-Perot cavity [J]. *Opt. Express*. 2006,**14**(20):9284-9292.

(下转第410页)

(电子)的影响较大,图中未显示出来. 该样品的迁移率非常低,77K 时只有 228 $cm^2/(V \cdot s)$,最大值在 55K 时为 251 $cm^2/(V \cdot s)$. 迁移率低的原因可能与样品退火激活过程中伴随产生 Te_{Hg} 有关. Te_{Hg} 易使周围晶格形成一个拉伸形变,而 Te_{Hg}-V_{Hg} 对则可能在材料中形成散射中心,使迁移率减小.

3 结论

从光学和电学两个方面研究了通用的两步退火后掺砷碲镉汞的性质. 光学和电学实验都表明经高温真空退火和低温富汞退火后的材料中存在 Te_{Hg} 和 Te_{Hg}-V_{Hg} 对,掺杂浓度越大,退火产生的 Te_{Hg}-V_{Hg} 对越多. Te_{Hg} 和 Te_{Hg}-V_{Hg} 对的存在降低了材料的迁移率.

REFERENCES

[1] REISINGER A R , ROBERTS R N, CHINN S R, *et al.* Photoluminescence of infrared-sensing materials using a FT-IR spectrometer, [J]. *Rev. Sci. Instrum.*, 1989, **60**(1): 82-86.

[2] HANSEN G. L., SCHMIDT J L, and CASSELMANT. N., Energy gap versus alloy composition and temperature in $Hg_{1-x}Cd_xTe$, [J]. *J. Appl. Phys.* 1982, **53**(10): 7099-7010.

[3] SHAO J, LU W, LV X *et al.* Modulated photoluminescence spectroscopy with a step-scan Fouriertransform infrared spectrometer, [J]. *Rev. Sci. Instrum.*, 2006, **77**(6): 063104-1-063104-6.

[4] SHAO J, YUE F Y, LV X *et al.* Phot-omodulated infrared spectroscopy by a step-scan Fourier transform infrared spectrometer, [J]. *Appl. Phys. Lett.* 2006, **89**(18): 182121-1-182121-3.

[5] LINDLE J R, BEWLEY W W, VURGAFTMAN I, *et al.* HgCdTe negative luminescence devices with high internal and external efficiencies in the midinfrared, [J]. *Appl. Phys. Lett.* 2007, **90**(24): 241119-1-241119-3.

[6] GARLAND J W, GREIN C H, YANG B. *et al.* Evidence that arsenic is incorporated as As_4 molecules in the molecularbeam epitaxial growth of $Hg_{1-x}Cd_xTe$: As, [J]. *Appl. Phys. Lett.* 1999, **74**(14): 1975-1978.

[7] AQARIDEN F, SHIH H D, KINCH MA, *et al.* Electrical properties of low-arsenic-doped HgCdTe grown by molecular beam epitaxy, [J]. *Appl. Phys. Lett.* 2001, **78**(22): 3481-3483.

[8] LEE T S., GARLAND J., GREIN C. H., *et al.* Correlation of arsenic incorporation and its electrical activation in-MBE HgCdTe, [J]. *J. Electronic Mat.* 2000, **29**(6): 869-872.

[9] Berding M. A., A. Sher, M. Van Schilfgaarde, *et al.* Modeling of arsenic activation in HgCdTe, [J]. *J. Electronic Mat.* 1998, **27**(6): 605-609.

[10] BOUKERCHE M, WIJEWARNASURIY-A P S, SIVANANTHAN S, *et al.* Th-e doping of mercury cadmium telluri-de grown by molecular-beam epitaxy, [J]. *J. Vac. Sci. Technol.* A, 1988, **6**(4): 2830-2833.

[11] SHAO J, CHEN L, LV X, *et al.* Realization of photoreflectance spectroscopyin very-long wave infrared of up to 20 μm, [J]. *Appl. Phys. Lett.* 2009, **95**(4): 041908-1-041908-3.

[12] ZHANG X H , SHAO J, CHEN L, *et al.* Infrared photoluminescence of arsenic-doped HgCdTe in a wide temperature range of up to 290 K [J]. *J. Appl. Phys.* 2011, 110 043503.

[13] SHAO J, CHEN L, LU W, *et al.* Backside-illuminated infrared photoluminescence and photore? ectance: Probe of vertical nonuniformity of HgCdTe on GaAs, [J]. *Appl. Phys. Lett.* 2010, **96**(12): 121915-1-121915-3.

[14] FINKMAN E , NOMINOVSKY Y, Electrical properties of shallow levels i-n p-type HgCdTe, [J]. *J. Appl. Phys.* 1986, **59**(4): 1205-1211.

[15] BERDING M A , SHER A, ArsenicIncorporation during MBE growth of HgCdTe, [J]. *Appl. Phys. Lett.* 1999. **74**(5): 685-687.

[16] SCOTT W, STELZER E L, HAGER R J. Electrical an far-infrared optical properties of p-type $Hg_{1-x}Cd_xTe$, [J]. *J. Appl. Phys.* 1976, **47**(4): 1408-1414.

[17] KENWORTHY I, CAPPER P, JONES C L, *et al.* Determination of accepto-r ionisation energies in Cd, Hg, -, Te, [J]. *Semicond. Sci. Technol.* 1990, **5**: 854-860.

[18] CHEN M C , TREGIIGAS J H, Th-e activation energy of copper shallow acceptors in mercury cadmium telluri-de [J]. *J. Appl. Phys.* 1987, **61**(2): 787-789.

(上接 392 页)

[5] Chung T , Rapaport A , Smirnov V , *et al.* Solid-state laser spectral narrowing using a volumetric photothermal refractive Bragg grating cavity mirror [J]. *Opt. Lett.* 2006, 31: 229-231.

[6] Igor Ciapurin, Vadim Smirnov , George Venus. High-power laser beam control by PTR Bragg gratings [C]. Proceedings of CLEO, 2004: CTuP51.

[7] Song Bao-an, Zhao Wei-jiang, Ren De-ming, *et al.* Smooth-pulse of the single longitudinal mode obtained with twisted mode and passive Q-switch [J]. Journal of Optoelectronics Laser. 2008, **19**(10): 1328-1331.

[8] Herwig Kogelnik. Coupled Wave Theory for thick Hologram Gratings [J]. *The Bell system technical Journal.* 1969, **48**(9): 2909-2949.

[9] Igor V Ciapurin, Leonid B Glebov, Vadim I Smirnov. Modeling of Gaussian beam diffraction on volume Bragg grating in PTR glass [C]. Proc. of SPIE, 2005, 5742: 183-194.

[10] He-yong Zhang, Wei-jiang Zhao, De-ming REN et al. Laser linewidth measurement based on image processing and non-air gap F-P etalon [C]. Proc. of SPIE, 2009, 7384: 1-8.